

1 **Title: Systems-level analysis of patients treated for acute *P. falciparum***
2 **malaria reveals a role for the humoral response and cytokine milieu in**
3 **limiting $\gamma\delta$ T cell expansion**

4 **Authors:** Maximilian Julius Lautenbach^{1,2}, Victor Yman^{1,3}, Nadir Kadri^{1,2,4}, David Fernando
5 Plaza^{1,2}, Sina Angenendt^{1,2}, Klara Sondén^{1,2}, Anna Färnert^{1,2}, Christopher Sundling^{1,2*}

6
7 **Affiliations:**

8 ¹Division of Infectious Diseases, Department of Medicine Solna, and Center for Molecular
9 Medicine, Karolinska Institutet, Stockholm, Sweden.

10 ²Department of Infectious Diseases, Karolinska University Hospital, Stockholm, Sweden.

11 ³Department of Infectious Diseases, South Stockholm Hospital, Stockholm, Sweden

12 ⁴Science for Life Laboratory, Department of Medicine Solna, Karolinska Institute.

13

14 *Corresponding author. Email: christopher.sundling@ki.se (C.S.)

15

16 **One Sentence Summary:** A systems immunology analysis on natural malaria sheds light on
17 disease tolerance mechanism associated with gamma delta T cell expansion (134/150 with
18 spaces)

19

20 **Abstract:**

21 The mechanism of acquisition and maintenance of natural immunity against *Plasmodium*
22 *falciparum* malaria remains unclear. Although, clinical immunity develops over time with repeated
23 malaria episodes, disease tolerance is more rapidly acquired compared to protective immunity. It
24 remains unclear, how pre-existing immune responses impacts the mechanism responsible for
25 disease tolerance. Here, we investigated a cohort of returning travelers treated for acute
26 symptomatic *P. falciparum* malaria, either infected for the first time, or with a previous history of
27 malaria. Through repeated sampling over one year in a malaria free setting, we were able to study
28 the acute and longitudinal effects of the infection. We combined comprehensive immune cell and
29 plasma protein profiling with integrated and data driven analysis, describing the immune landscape
30 from acute disease to one year after infection. We identified a strong association between pro-
31 inflammatory signatures and $\gamma\delta$ T cell expansion. The association was significantly impacted by
32 previous exposure to malaria, resulting in a dampened pro-inflammatory response, which
33 translated to reduced V δ 2⁺ $\gamma\delta$ T cell expansion compared to primary infected individuals. The
34 dampened inflammatory signal was associated with early expansion of Fc γ RIII⁺ monocytes and
35 parasite-specific antibodies of IgG1 and IgG3 isotypes.

36 Our data suggest that the interplay of Fc γ RIII⁺ monocytes and a cytophilic parasite-specific IgG
37 during the early blood stage infection lead to lower parasitemia and a dampened pro-inflammatory
38 response with reduced $\gamma\delta$ T cell expansion. This enhanced control and reduced inflammation points
39 to a potential mechanism on how tolerance is established following repeated malaria exposure.
40 (244/250 words)

41

42 **Main Text:**

43 **INTRODUCTION**

44 Malaria remains a global burden with an estimated 229 million malaria cases leading to
45 approximately 409 000 deaths in 2019 (1). Compared to other pathogens, immunity to malaria is
46 slow to develop (2). In malaria endemic areas, partial immunity is acquired over time after repeated
47 infections. Clinical symptoms are reduced while low grade subclinical infections remain and allow
48 for continued parasite transmission (2, 3). However, protection from severe forms of malaria,
49 despite high levels of parasitemia, seem to develop already after a few infections (4). A recent
50 study by Nahrendorf and colleagues suggests a tolerance mechanism where better control of host-
51 damaging factors that are part of the natural immune response to infection are an underlying cause
52 for the reduced severity (5). Currently no study has investigated how long tolerance persists and
53 how it is maintained in response to malaria.

54 Clinical symptoms are due to the blood stage of the infection, where merozoites invade
55 erythrocytes that then sequester, followed by parasite multiplication before bursting out to infect
56 new erythrocytes (6). The clinical manifestations are partly due to the strong innate pro-
57 inflammatory response, during the parasite blood stage/to the *P. falciparum* blood stage (7).

58 Much of our current understanding of the immune responses to *P. falciparum* infection is based
59 on hypothesis-driven research, where selected cell subsets, inflammatory markers, or clinical
60 features are investigated at a time (8, 9). Improved technology and bioinformatic tools enable the
61 analysis of high-dimensional parameters in limited sample material, giving us the opportunity to
62 study complex immune responses at a systems level to provide new insights into complex
63 immunological networks that represent the immune response during infection (10). Systems level
64 approaches to study febrile/non-febrile children in malaria endemic countries (11) as well as the
65 comparison of malaria naïve and Africans in controlled human malaria infection (CHMI) studies
66 (12) have generated valuable findings and new hypotheses. While studies in endemic populations
67 allow investigation of acute naturally acquired malaria and persistent (largely asymptomatic)
68 infections in the context of previous exposure. Despite CHMI studies enable more control over
69 prior parasite exposure, infectious dose, and follow-up after infection, although only in the context
70 of very low level parasitemia and often before symptoms having appeared. Although compensating
71 for some limitations, CHMI cannot fully mirror a natural infection, due to early treatment not
72 allowing observation of potential effects derived from a strong natural symptomatic infection. This

73 leaves a knowledge gap on how natural infection affects the immune response in the absence of
74 potential parasite re-exposure. This gap can be filled by investigating the immune response after
75 naturally acquired malaria in individuals leaving the endemic area, seeking healthcare in a setting
76 without risk of re-exposure.

77 Here, we study a prospective cohort of returning travelers treated for acute *P. falciparum* malaria
78 at the Karolinska University Hospital in Sweden, followed over one year after infection. Using a
79 systems immunology approach and data-driven analysis, we combined plasma protein and cell
80 profiling to study dynamic changes of the immune response over time in these patients. Based on
81 our results, we propose a model where antibody-derived memory modulates the pro-
82 inflammatory cytokine response which in turn impact $\gamma\delta$ T cell expansion and improve disease
83 tolerance.

84

85 RESULTS

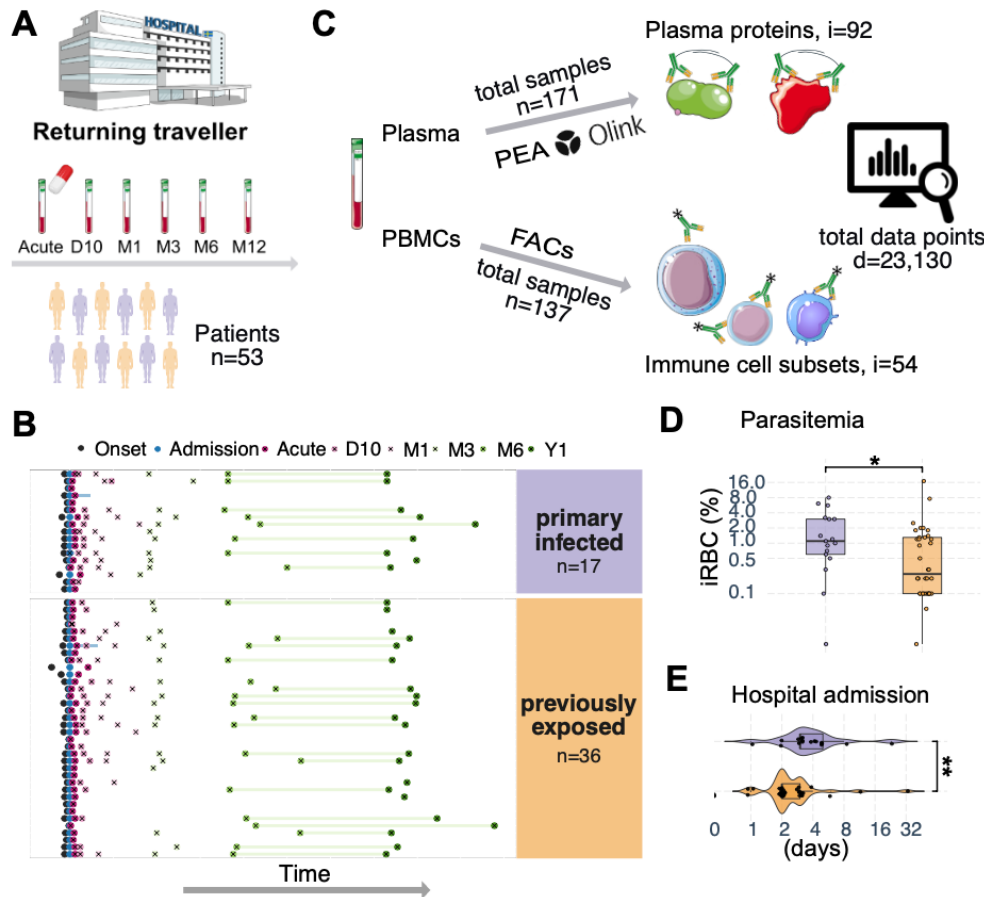
86 Subhead 1: Longitudinal profiling of peripheral blood – Immune dynamics after natural 87 infection in a cohort of returning travelers

88 We aimed to comprehensively profile the immune response dynamics longitudinally after natural
89 infection with *P. falciparum* malaria, to appreciate the immunological changes occurring during
90 the acute disease and up to one year after diagnosis. We included 53 returning travelers, repeatedly
91 sampled in a non-endemic setting over one year after hospital admission (13–16) (Fig. 1A).

92 To profile the immune response in the cohort over time, we performed broad FACS-based
93 immunophenotyping using a 17-marker panel and gated for subsets of monocytes (CD14⁺), T cells
94 (CD3⁺CD56⁻), and NK cell (CD3⁻CD56⁺) (Fig. S1A). We also included data from B cell subsets
95 previously phenotyped from the same donors (16) (Fig. S1B). Plasma protein analysis was
96 performed using the Target 96-plex Inflammation panel from Olink Proteomics (17) targeting 92
97 immune response-related proteins. In total, we profiled 182 samples from 53 subjects, creating
98 more than 23,000 data points (Fig. 1B).

99 The cohort consisted of individuals infected with *P. falciparum* malaria for the first time (primary
100 infected, n = 17) and those infected before, having grown up in malaria endemic areas and reported
101 previous malaria (previously exposed, n = 36) (Fig. 1C). Comparing individuals with primary
102 infection versus previous exposure enabled us to investigate potential memory effect on the
103 immune response. The individuals with previous exposure moved from malaria endemic areas to
104 non-endemic Sweden on average 11.5 years before now experiencing acute malaria after visiting
105 an endemic area (median = 11.5, range 0–46 years, Tab. S1).

106 Although all individuals sought healthcare, primary infected patients had significantly higher
107 levels of parasitemia at hospital admission (median 1.10 vs 0.25 % infected red blood cells, p =
108 0.038, Fig1D), more signs of severe malaria (Tab. S1) and were on average admitted to hospital
109 care significantly longer than previously exposed patients (median 3 vs 2 days, p = 0.002, Fig1E,
110 Tab. S1).



111

112 **Fig. 1. Systems level profiling of peripheral blood from individuals of a prospective cohort of**
 113 **returning travelers with *P. falciparum* malaria. (A) Overview of prospective longitudinal malaria**
 114 **cohort of returning travelers, (B) temporal sample information symptom onset (black), admission**
 115 **to Karolinska University Hospital (blue), six sampling time points (x) for immune profiling (acute,**
 116 **after 10 days, 1 month, 3 months, 6 months, 1 year) and convalescence average (green lines).**
 117 **Patients with primary infection (n = 17) are colored in purple, and patients with previous malaria**
 118 **exposure (n = 36) are colored in orange. (C) A total of 53 returning travelers were longitudinally**
 119 **profiled for plasma proteins using Olink Proteomics PEA platform (n = 171 samples, i = 92**
 120 **proteins) and their PBMC immune cells (n = 137 samples, i = 54 subsets), generating 23,130**
 121 **unique data points. Comparison of (D) parasitemia at diagnosis (percentage of infected red blood**
 122 **cells) and (E) length of hospital admission (days) for primary infected and previously exposed**
 123 **individuals. Statistical differences between groups were assessed using the non-parametric**
 124 **Wilcoxon-test. *p < 0.05, **p < 0.01.**

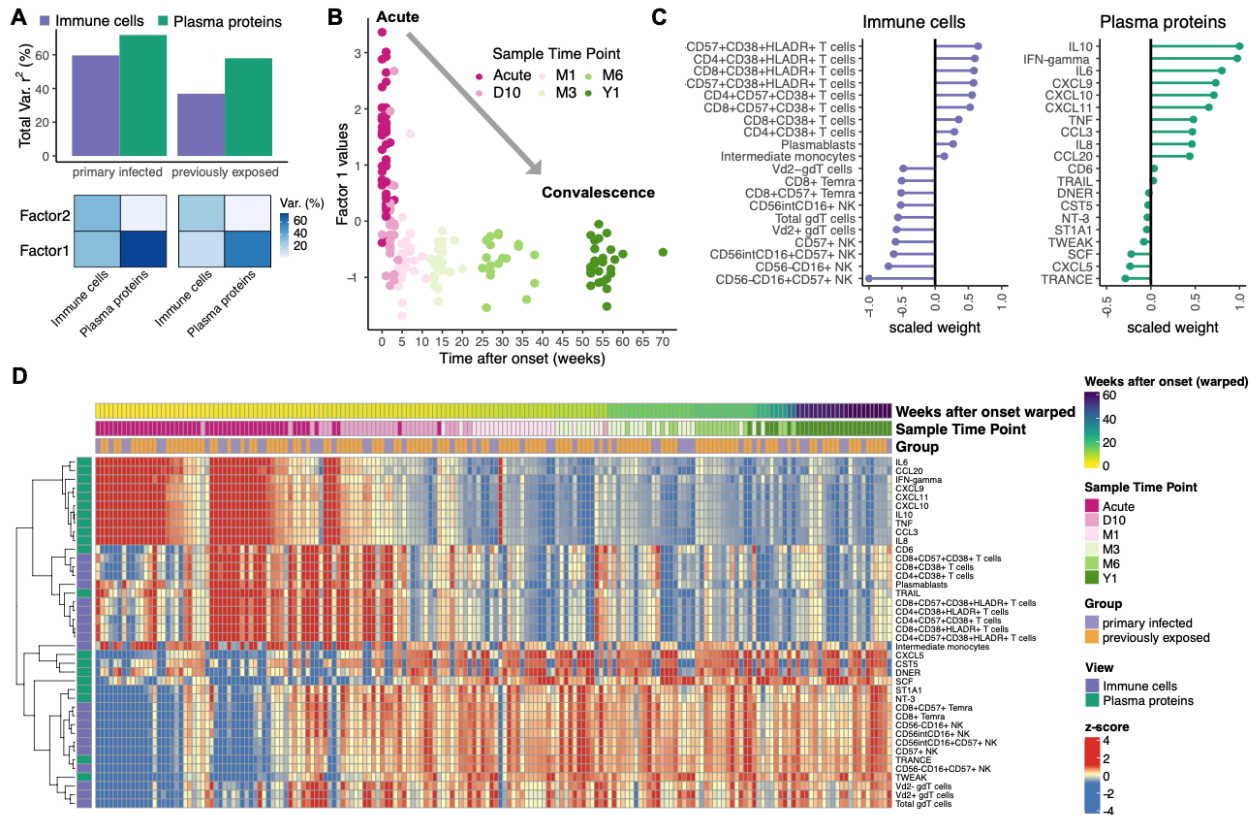
125

126 **Subhead 2: Integrated analysis of immune response on time axis after symptom onset**

127 To explore the immune response dynamics after natural *P. falciparum* malaria on a systems level
128 and in a data driven manner, we used multi-omics factor analysis (MOFA). The unsupervised
129 nature of MOFA allows the model to capture both biological and technical variability in the low-
130 dimensional factors space (18, 19). Here we used MEFISTO, a recent extension of MOFA which
131 allows for multi-omics integration of data while controlling for time-dependent variance in
132 repeated samples (20). MOFA can disentangle the sources of heterogeneity in diverse data types
133 and accept missing data points using matrix factorization (Fig. S2A). Using MEFISTO, the dataset
134 was described by two latent factors. These factors explained 37% to 60% and 58% to 72 % of the
135 immune cell subset and plasma protein dynamics, respectively (Fig. 2A). Factor1 was primarily
136 associated with time-dependent changes in the immune response to the infection (Fig. 2B and
137 S2B). Positive factor values were associated with the acute phase and negative factor values were
138 associated with the time after treatment and transition towards convalescence (Fig. 2B and S2C).
139 The positive factor values were driven by increased levels of IL10, pro-inflammatory cytokines
140 such as IFN-gamma, IL-6, TNF, CCL3, IL8, CDCP1, and chemokines such as CXCL9, CXCL10,
141 CXCL11. For immune cells, CD4⁺ and CD8⁺ T cells expressing activation markers CD38 and
142 HLA-DR, intermediate monocytes (CD14⁺CD16⁺) and plasmablasts
143 (CD19⁺CD20^{lo}CD38^{hi}CD27^{hi}) were associated with Factor1 (Fig. 2C). The negative factor values
144 were associated with the transition phase towards convalescence. Here, several subsets of NK cells
145 expressing CD57, CD8 T effector memory cells, and $\gamma\delta$ T cells were variables driving Factor1 for
146 the cellular immune response after treatment (Fig. 2C). We confirmed the accuracy of the model
147 parameters by comparing measured data between the acute and convalescent samples (internal
148 control; Fig. S2C-F) and to healthy control samples (external control; Fig. S3A-D).

149 We then used the integrated MEFISTO model to impute missing data points (plasma proteins data
150 modality, n = 11; immune cell modality, n = 64; Fig. S2A) to generate a heatmap of the integrated
151 immune landscape, visualizing the longitudinal immune system dynamics after disease. The
152 landscape dynamics, show a rapidly contracting pro-inflammatory response after treatment with a
153 temporary increase in primarily activated T cell subsets followed by a transition into a more long-
154 term post-infection response (Fig. 2D and Fig. S3).

155 In summary, our integrated analysis of immune cell subsets and plasma protein data after symptom
 156 onset allows us to draw a data driven descriptive immune landscape, describing the transition from
 157 the clinical acute phase towards convalescence over one year.
 158



159
 160 **Fig. 2. Integrated analysis of immune response dynamics for one year after malaria.** Integrated
 161 multi omics factor analysis method for the Functional Integration of Spatial and Temporal Omics
 162 data (MEFISTO) model was utilized to integrate data modalities, plasma proteins and manually
 163 gated cell subsets, respectively, with their temporal covariate of time after symptom onset. (A)
 164 Variance explained by the MEFISTO model. Differences due to previous parasite exposure were
 165 assigned to groups in order to model group-specific time-dependent immune response dynamics.
 166 (B) Plotting Factor1 value against the time after symptom onset (weeks) highlights the captured
 167 variance in Factor1 with positive factor values associated with acute phase samples and negative
 168 factor values associated with non-acute phase samples. (C) Top10 features of Factor1 for each of
 169 the immune system views based on negative and positive scaled feature weights - immune cells
 170 (purple) and plasma proteins (green). (D) The heatmaps visualize immune response dynamics for

171 *Factor1 driving features. The characteristic immune variables for each data modality, aligned to*
172 *time after symptom onset, reveals contrasting patterns characterizing the transition from acute*
173 *phase towards convalescence. Missing data points have been imputed based on model Factor1.*
174 *Cell counts and relative protein levels are shown as rows, and each column represents an*
175 *individual patient. Rows were clustered using Euclidean distance and column were arranged*
176 *according to MEFISTO model group-aligned time after onset. Cell counts and protein level values*
177 *were converted to z-scores.*
178

179 **Subhead 3: Relationship between acute cytokine milieu and cellular response**

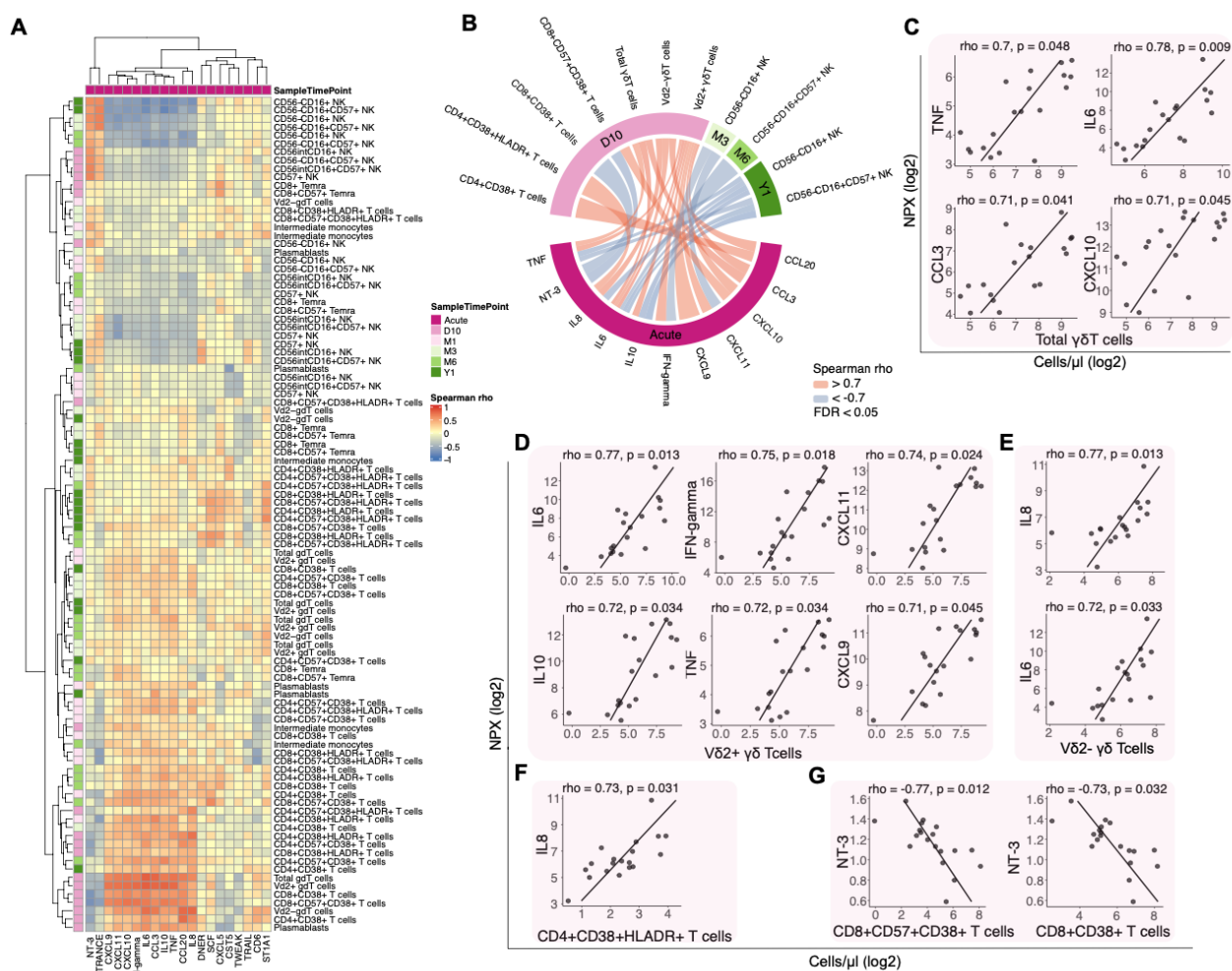
180 Cytokines and chemokines are known to orchestrate an immunological response to drive
181 recruitment, activation, and subsequently proliferation of immune cell populations. Hence, we
182 sought to analyze possible associations between levels of the acute phase responses and immune
183 cells subsets, characterizing the transition from acute towards convalescence.

184 Focusing on the top immune variables determined by the integrated model, we correlated acute
185 samples with all remaining sample time points using spearman rank correlation (Fig. 3A). We
186 discovered strong and significant correlations ($|\rho| > 0.7$, after adjusted FDR < 0.05) between
187 acute phase cytokines and immune cell subsets at all sample time points after treatment (D10, M3,
188 M6 and Y1) (Fig. 3B).

189 In particular, the numbers of $\gamma\delta$ T cell subsets at the 10-day sample time-point were strongly
190 associated with several pro-inflammatory cytokines at the acute time-point. The total level of
191 $\gamma\delta$ T cells positively correlated with TNF ($\rho = 0.704$, $p = 0.049$), IL6 ($\rho = 0.781$, $p = 0.009$),
192 CCL3 ($\rho = 0.712$, $p = 0.041$), and CXCL10 ($\rho = 0.707$, $p = 0.045$) (Fig. 3C). Especially the
193 $V\delta 2^+$ subset of $\gamma\delta$ T cells has been shown to be important in the immune response to malaria
194 parasites (21–23). When investigating these subsets, we observed that the number of $V\delta 2^+$
195 $\gamma\delta$ T cells was positively correlated with levels of IL6 ($\rho = 0.767$, $p = 0.013$), IFN-gamma (ρ
196 $= 0.753$, $p = 0.018$), CXCL11 ($\rho = 0.74$, $p = 0.024$), IL10 ($\rho = 0.723$, $p = 0.034$), TNF ($\rho =$
197 0.724 , $p = 0.034$), and CXCL9 ($\rho = 0.707$, $p = 0.045$) (Fig. 3D). The number of $V\delta 2^-$ $\gamma\delta$ T cells
198 in contrast was only positively correlated with levels of IL8 ($\rho = 0.77$, $p = 0.013$), and IL6 (ρ
199 $= 0.72$, $p = 0.033$) (Fig. 3E).

200 Acute phase levels of IL8 were also positively correlated with the number of activated
 201 (CD38⁺HLA-DR⁺) CD4⁺ T cells ($\rho = 0.728$, $p = 0.031$) at the 10-day sample time-point. In
 202 contrast, neurotrophin-3 (NT-3) levels were negatively correlated with the number of activated
 203 CD8⁺ T cells in several different subsets (CD57⁺CD38⁺; $\rho = -0.77$, $p = 0.012$ and
 204 CD57⁺CD38⁺HLA-DR⁺; $\rho = -0.726$, $p = 0.042$) (Fig. 3F, G).

205 These results point towards a strong association of the levels of pro-inflammatory cytokines during
 206 the early acute phase and the size of immune cell subsets after the acute phase. The highest degree
 207 of association was identified for $\gamma\delta$ T cells, and especially the V δ 2⁺ subset, which was strongly
 208 positively correlated with the levels of pro-inflammatory cytokines.



209
 210 **Fig. 3. Associations of the acute phase plasma protein response with immune cell subsets. (A)**
 211 **Heatmap based on overall Spearman correlation (ρ) acute phase plasma proteins and post-**

212 acute phase cell immune cell subsets. Blue and red colors symbolize positive and negative
213 correlations, respectively. **(B)** Chord diagram based on strong ($\rho > |0.7|$) and significant
214 correlations values (after adjusted FDR < 0.05). **(C-G)** Scatter plots to show acute phase plasma
215 protein levels and immune cell subset counts at day 10 post disease for significant correlations of
216 **(C)** Total $\gamma\delta$ T cells, **(D)** $V\delta 2^-$ $\gamma\delta$ T cells, **(E)** $V\delta 2^+$ $\gamma\delta$ T cells, **(F)** activated $CD4^+$ T cells and **(G)**
217 activated $CD8^+$ T cells. All stated p -values are FDR corrected for multiple testing.

218

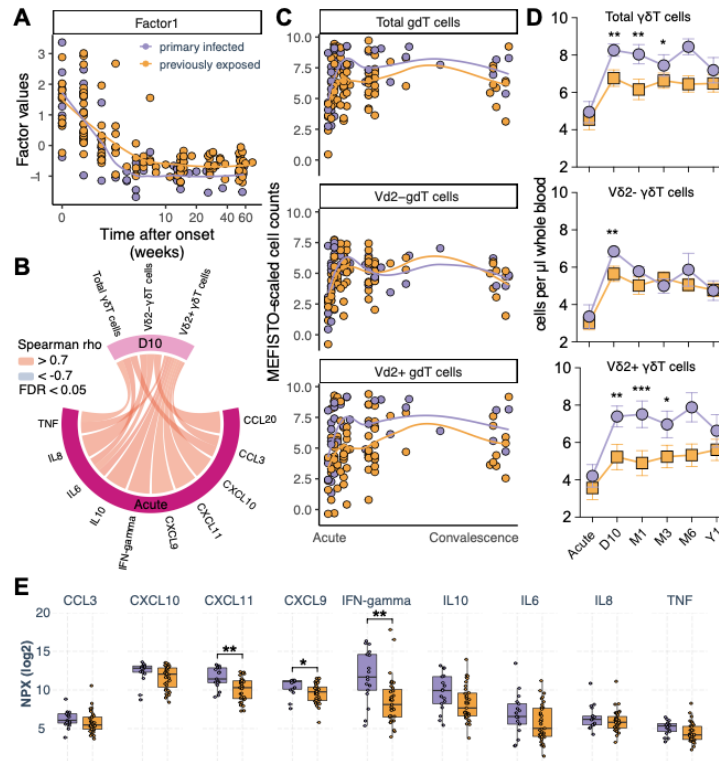
219 **Subhead 4: Impact of previous *P. falciparum* exposure on $\gamma\delta$ T cell responses**

220 To further characterize the association between acute phase cytokine levels and the $\gamma\delta$ T cell
221 response, we sought to examine if previous exposure to malaria parasites impacts this association.
222 Overall, both groups show similar trajectories of their immune dynamics when plotting Factor1
223 values against time (Fig. 4A). However, primary infected individuals were associated with both
224 higher and lower factor values during the acute phase and convalescent phase, respectively (Fig.
225 S2C). This indicates differences in protein and immune cell subset magnitudes attributed to
226 previous malaria.

227 Due to the strong correlation of acute phase proteins and $\gamma\delta$ T cell subset numbers at day 10 (Fig.
228 4B, excerpt of Fig. 3B), we aimed to investigate the association further in the context of previous
229 exposure.

230 When plotting $\gamma\delta$ T cells against the time after symptom onset, we observed that $V\delta 2^+$ $\gamma\delta$ T cells
231 expanded to a greater extent in primary infected individuals while $V\delta 2^-$ $\gamma\delta$ T cells expanded
232 similarly for both groups (Fig. 4C). We confirmed that especially the $V\delta 2^+$ subset was significantly
233 more expanded after the acute time-point in primary infected individuals (Fig. 4D). All acute phase
234 proteins that correlated with $V\delta 2^+$ $\gamma\delta$ T cells (Fig. 4B) followed a similar trend, although only IFN-
235 gamma, CXCL9 and CXCL11 were significantly higher in primary infected compared to
236 previously exposed individuals (Fig. 4E).

237 Here, we could show that primary infected individuals have significantly higher levels of pro-
238 inflammatory cytokines at the acute phase, as well as a significantly larger expansion of
239 $V\delta 2^+$ $\gamma\delta$ T cells after the acute phase compared with individuals previously exposed to malaria.



240

241 **Fig. 4. Impact of previous *P. falciparum* exposure on immune dynamics after clinical malaria.**

242 (A) Smooth fit of MEFISTO Factor1 values against time after symptom onset in weeks visualizing

243 transition from acute to convalescence for primary infected (purple) and previously exposed

244 (orange) individuals. (B) Associated inflammatory signature with $\gamma\delta$ T cells based on spearman

245 rank correlation. (C) $\gamma\delta$ T cell dynamics over time after symptom onset. (D) Longitudinal $\gamma\delta$ T cell

246 levels. Statistical differences between groups for $\gamma\delta$ T cell subtypes were assessed using linear

247 mixed model fit with restricted maximum likelihood and t-tests with FDR correction for multiple

248 testing. Error bars denote standard error of the mean. (E) Comparison between primary infected

249 (purple) and previously exposed (orange) individuals for acute phase proteins significantly

250 associated with $\gamma\delta$ T cells at the acute time-point. Statistical differences between groups were

251 assessed using the non-parametric Wilcoxon-test, FDR adjusted p-values to correct for multiple

252 testing. * $p < 0.05$, ** $p < 0.01$, *** $p < 0.001$.

253

254 **Subhead 5: Effect of previous malaria exposure on V δ 2⁺ $\gamma\delta$ T cell characteristics**

255 The V δ 2⁺ subset of $\gamma\delta$ T cells have been shown to play an important role in combating blood stage
256 malaria, via TCR-induced cytotoxicity and CD16 mediated phagocytosis (24, 25). We therefore
257 focused on characterizing the CD16⁺V δ 2⁺ $\gamma\delta$ T cell response further using linear-mixed effects
258 models to assess the impact of previous exposure to parasites on $\gamma\delta$ T cell functional markers.

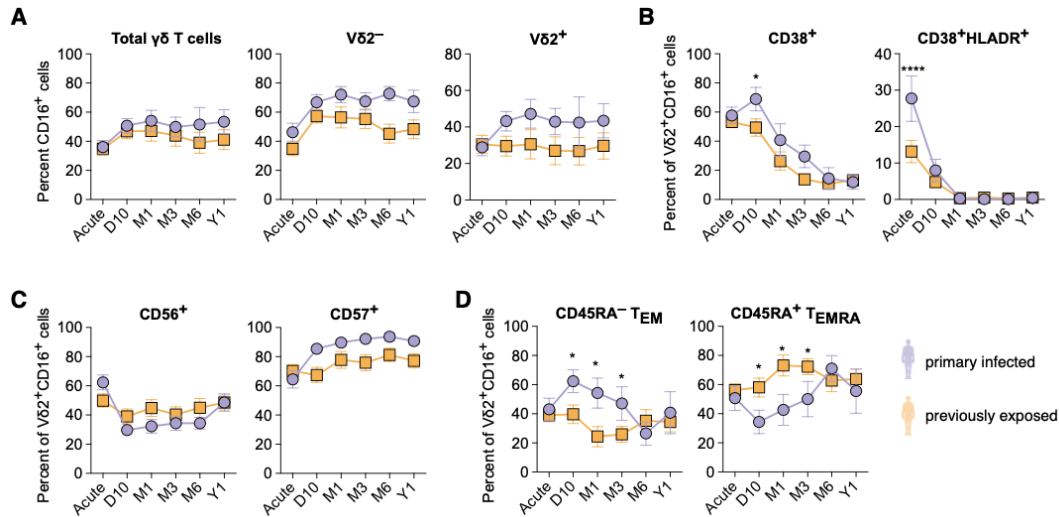
259 First, we assessed CD16 expression among $\gamma\delta$ T cells. The expression was similar between primary
260 infected and previously exposed individuals for total and V δ 2 positive and negative subsets (Fig.
261 5A). The frequency of CD16⁺ cells increased somewhat in both groups between the acute time-
262 point and 10 days, for V δ 2⁻ cells. A similar expansion was also observed for the V δ 2⁺ cells, but
263 only in primary infected individuals (Fig. 5A), potentially reflecting an upregulation in response
264 to infection. To further assess if the V δ 2⁺ $\gamma\delta$ T cells responded to the infection, we next investigated
265 the activation status of the CD16⁺V δ 2⁺ $\gamma\delta$ T cells. Approximately 60 % of all V δ 2⁺ $\gamma\delta$ T cells had
266 upregulated the activation marker CD38 at the acute infection. The primary infected individuals
267 then retained a significantly higher frequency of CD38⁺ cells at the day 10 time-point after which
268 the levels reduced over 3-6 months until reaching baseline levels (Fig. 5B). The increased
269 activation-status in primary infected individuals was also reflected by a significantly higher co-
270 expression of CD38 and HLA-DR at the acute time-point (Fig. 5B).

271 We also assessed the expression of CD56 and CD57, associated with NK cell cytotoxicity (26)
272 and replicative senescence (27), respectively. Although there were no differences between the
273 groups, there were some changes in cells expressing the markers over time, such as a temporary
274 reduction in the frequency of CD56⁺ cells after the acute infection, while CD57⁺ cells increased
275 over time (Fig. 5C). These effects were especially observed in primary infected individuals,
276 potentially reflecting the stronger $\gamma\delta$ T cell response in these individuals.

277 To further determine which subsets of V δ 2⁺ $\gamma\delta$ T cells that responded during infection, we assessed
278 the levels of CCR7 and CD45RA to identify different naïve or effector populations (28). Almost
279 all CD16⁺ V δ 2⁺ $\gamma\delta$ T cells were negative for CCR7 (median 98 % over all time-points), indicating
280 that these cells display an effector-phenotype. During the acute phase of the response, both groups
281 displayed similar distribution of effector memory (T_{EM}, CD45RA⁻) and T_{EMRA} (CD45RA⁺)
282 $\gamma\delta$ T cells (Fig. 5D). However, as the number of V δ 2⁺ $\gamma\delta$ T cells expanded in primary infected
283 individuals the frequency of effector memory cells significantly increased, while the frequency in

284 previously exposed individuals was relatively stable over time. This suggests that it was primarily
 285 effector memory $V\delta 2^+$ $\gamma\delta$ T cells that expanded after the acute infection.

286 Collectively these results show that despite $V\delta 2^+$ $\gamma\delta$ T cells only expanding in primary infected
 287 individuals, the cells became activated in both groups after infection. The level of activation and
 288 subsequent changes in host effector and differentiation markers were however different with a
 289 more robust effect in primary infected individuals.



290

291 **Fig. 5. Previous *P. falciparum* exposure impacts $\gamma\delta$ T cell expansion.** Linear mixed effect
 292 modelling by maximum likelihood for $\gamma\delta$ T cell frequencies for primary infected (purple) and
 293 previously exposed (orange) individuals, error bars denote the standard error of the mean. (A)
 294 Percentage of $CD16^+$ cells of total $\gamma\delta$ T cells, $V\delta 2^-$ or $V\delta 2^+$ $\gamma\delta$ T cells. (B) Percent of $V\delta 2^+$ $CD16^+$ $\gamma\delta$
 295 T cells expressing activation markers $CD38$ alone or together with $HLA-DR$. (C) Percent of $V\delta 2^+$
 296 $CD16^+$ $\gamma\delta$ T cells expressing $CD56^+$ or $CD57^+$ (D) $V\delta 2^+$ $\gamma\delta$ T cells effector memory ($CD45RA^-$) or
 297 T_{EMRA} ($CD45RA^+$). Difference in cell frequency at each time point was evaluated by repeated *t*-
 298 tests with FDR correction. **p* < 0.05, *****p* < 0.0001.

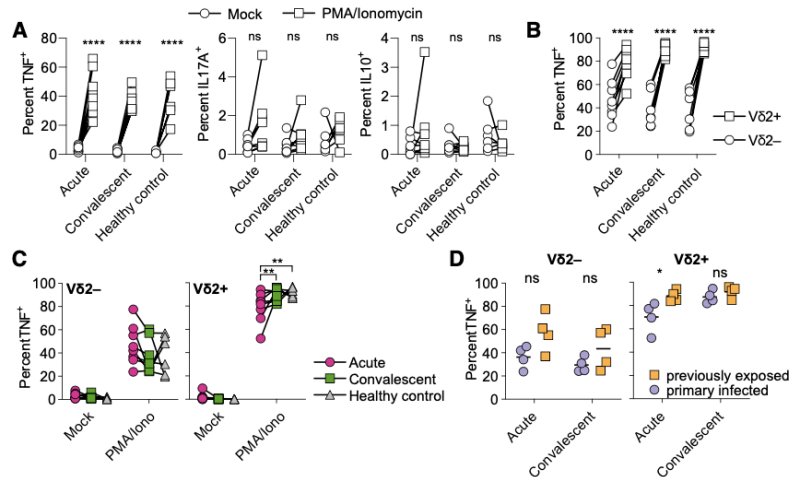
299

300 Subhead 6: $\gamma\delta$ T cell function is retained while expansion is affected due to previous 301 malaria exposure

302 It has been described that especially $V\delta 2^+$ $\gamma\delta$ T cells respond strongly during malaria but that this
 303 effect is reduced upon subsequent infections (29). This pattern is supported by our data, as the
 304 $V\delta 2^+$ $\gamma\delta$ T cell activation and especially expansion were reduced in previously exposed compared

305 to primary infected individuals (Fig. 4D). Previous descriptions indicate that the reduced
306 responsiveness can be due to changes in the imprinting through changes in the methylation patterns
307 (30, 31), although it remains unclear if such imprinting can last for this long. To assess if the
308 function of the $\gamma\delta$ T cells in our cohorts were inherently affected in their capacity to respond to
309 stimulation, we performed blinded cultures of PBMCs from primary infected and previously
310 exposed individuals. We stimulated the cells with PMA and ionomycin that together bypass the T
311 cell receptor complex and measured production of TNF α , IL17, and IL10. PMA and ionomycin
312 stimulation led to increased production of TNF α , but not IL17 or IL10 (Fig. 6A). Comparing the
313 response of V δ 2⁺ and V δ 2⁻ $\gamma\delta$ T cells, the V δ 2⁺ cells responded with more TNF α production (Fig.
314 6B), consistent with a proinflammatory effector function. For V δ 2⁻ $\gamma\delta$ T cells, the production of
315 TNF α was similar between the acute and convalescent time-point and healthy controls. For V δ 2⁺
316 $\gamma\delta$ T cells, however, the frequency of TNF α producing cells was reduced during the acute response,
317 but then recovered at the convalescent phase, for which frequencies were similar as in healthy
318 controls (Fig. 6C). Further separating the V δ 2⁺ and V δ 2⁻ subsets into primary infected and
319 previously exposed individuals showed no differences between the groups for V δ 2⁻ cells, while
320 primary infected individuals responded with lower numbers of TNF α -producing V δ 2⁺ cells at the
321 acute time-point (Fig. 6D), potentially reflecting a larger proportion of already activated cells being
322 restimulated.

323 In summary, V δ 2⁺ $\gamma\delta$ T cells from previously exposed individuals do not display apparent intrinsic
324 dysfunctionality upon *ex vivo* reactivation. This further supports a role for extrinsic factors
325 regulating V δ 2⁺ $\gamma\delta$ T cell activation and expansion in malaria.



326

327 **Fig. 6. $\gamma\delta$ T cell function in response to restimulation.** (A) PBMCs from donors with primary
 328 infection ($n = 4$) and previous parasite exposure ($n = 4$) at the acute and convalescent time-point
 329 (6-12 months after infection) and healthy controls ($n = 6$) were stimulated with PMA and
 330 ionomycin (open boxes) or left unstimulated (Mock, open circles) for 5 hours. Frequencies of
 331 TNF α , IL17A, and IL10-producing cells were then measured. (B) TNF $^+$ cells were compared
 332 between V $\delta 2^+$ (open boxes) and V $\delta 2^-$ (open circles) cell subsets. (C) Comparison of TNF $^+$
 333 frequencies in V $\delta 2^-$ and V $\delta 2^+$ cell subsets at the acute time-point (pink circles), convalescent time-
 334 point (green boxes) and healthy controls (grey triangles). (D) Comparison of TNF $^+$ V $\delta 2^-$ and V $\delta 2^+$
 335 cells between primary infected (purple circles) and previously exposed (orange boxes) individuals.
 336 Statistical comparisons for A-C were done using a matched pair two-way ANOVA followed by
 337 Tukey's post-hoc test, while statistics in D was evaluated by two-way ANOVA followed by Sidak's
 338 post-hoc test. * $p < 0.05$, ** $p < 0.01$, *** $p < 0.0001$, ns = not significant.

339

340 **Subhead 7: Acute malaria specific IgG3 levels are associated with the level of inflammation** 341 **and $\gamma\delta$ T cell expansion**

342 A long-lived memory imprint to pathogenic encounter is in general mediated by the adaptive
 343 immune system. Here, we report that previously exposed individuals without re-exposure to
 344 parasites for many years (average 11.5 years since leaving an endemic region), at the time of a
 345 new acute infection respond with a reduced pro-inflammatory cytokine response upon re-infection
 346 as well as reduced V $\delta 2^+$ $\gamma\delta$ T cell expansion. Hence, we hypothesized that the reduced pro-

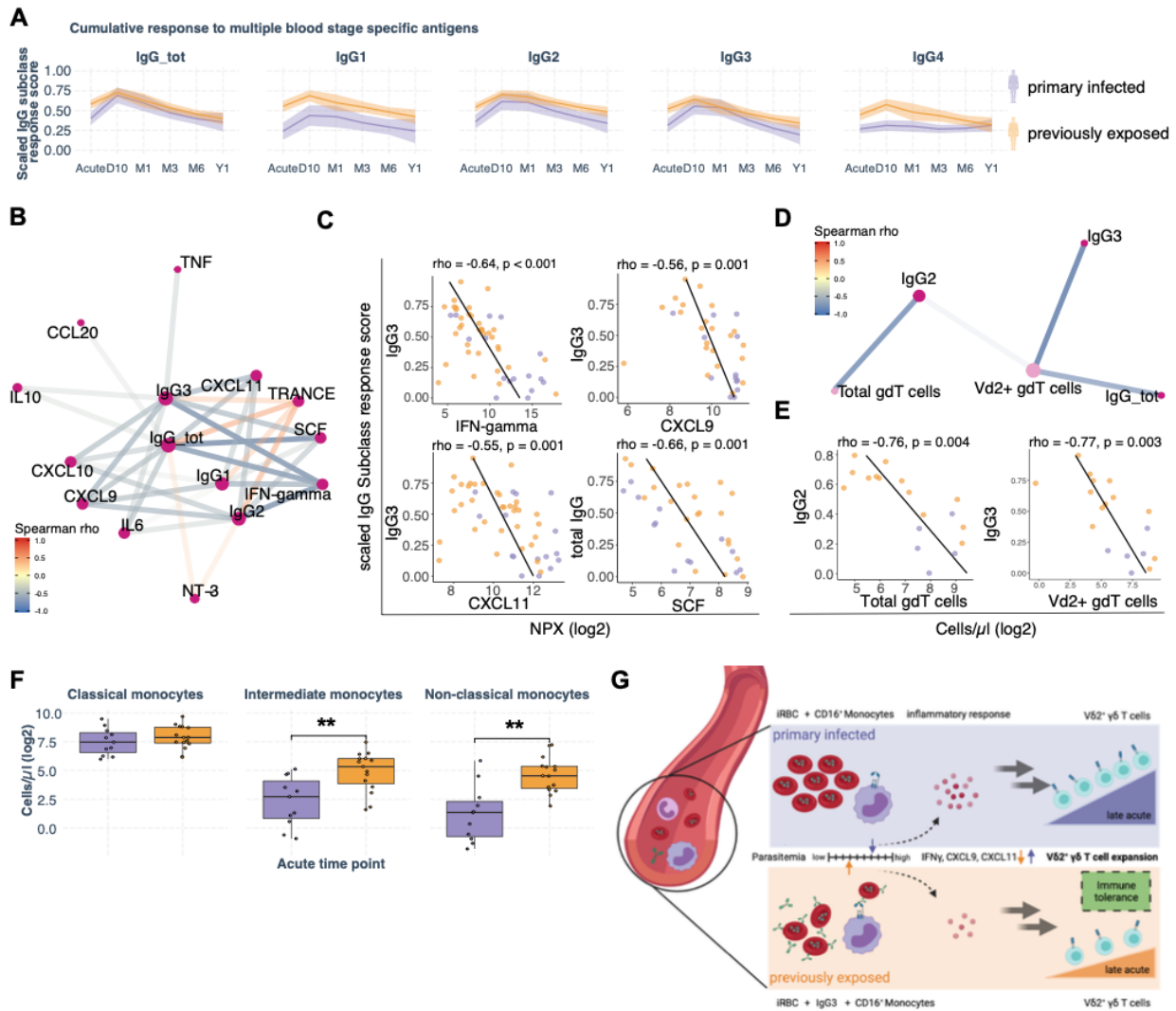
347 inflammatory response and $\gamma\delta$ T cell expansion could be mediated by existing long-lived adaptive
348 humoral immune memory responses.

349 To investigate this, we repurposed a previously published dataset, investigating the
350 immunoglobulin G subclass response (IgG1-4) to five malaria *P. falciparum* blood-stage antigens
351 (AMA1, MSP1, MSP2, MSP3, and RH5) in 51 matching individuals from the same cohort (15).
352 We established an IgG subclass and time point specific score, the cumulative response score (CRS)
353 that summarizes the responses to the separately measured malaria specific antigens from the
354 previous study (Fig. S5). The CRS dynamics correspond to the average breadth of the antibody
355 response for total IgG and IgG subclasses (Fig. 7A).

356 Spearman rank correlation showed that levels of several acute pro-inflammatory cytokines were
357 strongly inversely correlated with IgG subclass CRS (Fig.7B), in particularly IgG3 and IFN-
358 gamma levels (Fig. 7C). The IgG2 and IgG3 subclass CRSs at the acute infection were also
359 negatively correlated with day 10 total and $V\delta 2^+$ $\gamma\delta$ T cell numbers, respectively (Fig. 7D), with
360 an especially strong negative correlation between IgG3 levels and $V\delta 2^+$ $\gamma\delta$ T cell numbers (Fig.
361 7E).

362 Cytophilic immunoglobulins such as IgG3 can interact with CD16 expressing immune cells,
363 including $\gamma\delta$ T cells, and intermediate ($CD16^+CD14^{high}$) and non-classical ($CD16^+CD14^{lo}$)
364 monocytes. Interestingly, we observed higher numbers of intermediate and non-classical
365 monocytes at the acute time point for previously exposed compared to primary infected individuals
366 (Fig. 7F). These observations, together with an increased IgG3 response, points towards an
367 antibody-phagocytosis mediated mechanism that could partly explain the lower parasitemia
368 observed in individuals with prior exposure to malaria parasites (Fig. 1E). To assess if this could
369 be the case, we used linear regression to determine which associated combinations of immune
370 factors that best explain the difference in expansion of $V\delta 2^+$ $\gamma\delta$ T cells for the two exposure groups.
371 Using Directed Acyclic Graphs (DAG) (32), we determined the minimal sufficient adjustment sets
372 of covariates for estimating the total effect of a given associated component on acute IFN-gamma
373 levels and day 10 $V\delta 2^+$ $\gamma\delta$ T cell numbers, respectively (described in Supplementary Methods and
374 Fig. S7). Comparing the reference model with exposure group as explanatory variable to the DAG-
375 based adjusted immune response component model, we concluded that the IFN-gamma response
376 was not directly explained by the parasitemia (Fig. S7A). In contrast, differences in $V\delta 2^+$ $\gamma\delta$ T cell

377 expansion was partly explained by parasitemia, but more directly by cytophilic antibody levels
 378 and CD16⁺ intermediate monocytes (Fig. S7B-C). This suggests a potentially more direct
 379 antibody-mediated effect by regulating cytokine levels. Based on these results we suggest a
 380 working model where early production of parasite-specific antibodies interact with innate immune
 381 cells to regulate parasitemia and cytokine levels, which in turn control subsequent $\gamma\delta$ T cell
 382 expansion (Figure 7G).
 383



384
 385 **Fig. 7. Adaptive response due to prior malaria exposure linked to dampened immune**
 386 **inflammation.** (A) Cumulative IgG subclass response score (CRS) to 5 blood-stage antigens from
 387 Yman et al., BMC Medicine, 2019, over sample time points for primary infected (purple) and

388 *previously exposed (orange) individuals (n = 52), shaded area denotes the 95% confidence*
389 *interval. (B) Correlation network of plasma proteins and IgG subclass CRS values at the acute*
390 *time-point, FDR corrected $p < 0.05$ (C) Scatter plots for significant correlations, FDR adjusted p -*
391 *values are stated. (D) Correlation network of acute IgG subclass CRS values and immune cell*
392 *subsets at the 10-day sample time point, FDR corrected $p < 0.05$, $\rho < -0.7$. (E) Scatter plots for*
393 *significant correlations, FDR corrected $p < 0.05$. (F) Cell counts of monocyte subsets at the acute*
394 *time point. Statistical differences between groups were assessed using the non-parametric*
395 *Wilcoxon-test, FDR adjusted p -values to correct for multiple testing. $*p < 0.05$, $**p < 0.01$ (G)*
396 *Schematic model to explain improved disease tolerance in previously exposed individuals.*

397 **DISCUSSION**

398 Immunity to malaria is slow to develop. It has been proposed that this is partly due to immune
399 perturbations during infection (41). Understanding how the immune system is affected during
400 natural infection with malaria parasites is important to identify the potential role of individual
401 immune mediators in this process. Here, we used systems immunology to comprehensively
402 investigate the immune landscape after natural malaria and over one year after infection in the
403 absence of re-exposure to parasites. By sampling each individual over time, we could reduce
404 potential noise associated with inter-individual variability in their immune response to the
405 infection. Overall, the integrated immune landscape identified the acute phase followed by a
406 transitional phase leading into convalescence up to one year after disease. The acute phase was
407 characterized by activated CD4⁺ and CD8⁺ T cells and high levels of inflammatory cytokines and
408 chemokines, consistent with previous literature (2, 33). Here, a comprehensive analysis of immune
409 components over time revealed that acute inflammatory response signature associated with long-
410 term changes to cellular immune response.

411
412 The composition of our cohort, consisting of both primary infected and previously exposed
413 individuals, allowed us to study the impact of memory on the acute response and its associations
414 with the transition towards immunological convalescence. We could show that previously exposed
415 individuals produce lower levels of pro-inflammatory cytokines during natural *P. falciparum*
416 infection. Similar findings have been observed at the blood transcriptome level by Tran et al.,
417 where Malian adults exhibited a dampened inflammatory response compared to first time CHMI-
418 infected Dutch adults (34). Further, a study from a cohort of children in Uganda showed that older
419 children have lower levels of serum cytokines during acute malaria compared to younger children
420 (35). These previous studies, together with our findings of reduced pro-inflammatory response
421 confirms that previous malaria exposure, possibly cumulative, induces a form of tolerance
422 response. Of note, all individuals in our cohort experienced clinical malaria, suggesting that the
423 level of tolerance could be dependent on the amount of prior exposure to the parasite. However,
424 the individuals with previous exposure had left malaria endemic areas on average 11.5 years earlier
425 before being reinfected/experiencing a new episode of acute *P. falciparum* malaria after visiting
426 endemic area, indicating that the mechanism is significantly long-lived.

427

428 Antibodies are highly associated with protection from malaria and a key building block of naturally
429 acquired immunity. We have recently reported that previously exposed individuals from our cohort
430 responded to infection by producing high levels of *P. falciparum*-specific IgG, particularly of the
431 cytophilic subclasses IgG1 and IgG3 (15). Memory B cells and long-lived plasma cells constitute
432 a likely source of the increased parasite specific antibodies (15, 36), as memory can be maintained
433 for up to 16 years without re-exposure in a different cohort of travelers (37). Re-purposing the
434 previously published antibody data (15) enabled us to link the effect of adaptive responses, in the
435 form of an increased cytophilic antibodies, to enhanced functionality of the innate response. As
436 reported here, previously exposed individuals responded to malaria with an overall dampened
437 inflammatory response but significantly higher numbers of intermediate monocytes (38). Their
438 expression of CD16 (FcγRIII), a receptor for cytophilic antibodies of the subclasses IgG1 and
439 IgG3, can mediate parasite clearance through antibody-dependent phagocytosis (ADP) and/or
440 antibody-dependent cellular cytotoxicity (ADCC) (39). Indeed, higher numbers of CD16⁺
441 monocytes and a stronger IgG3 response against blood stage antigens indicate an interplay which
442 could promote lower levels of parasitemia, compared to individuals without previous exposure.
443 Supporting such a mechanisms, vaccination with RTS,S/AS01 leads to CD16-mediated
444 phagocytosis associated with protection (40).

445

446 We propose that antibody-mediated parasite control is an important component in shaping the pro-
447 inflammatory cytokine milieu towards a reduced pro-inflammatory response which could be
448 important for the development of immune tolerance (41). Complementary to the described
449 adaptive-innate interplay, several recent studies suggest that monocytes are modulated towards a
450 tolerance phenotype (5, 41). The mechanism of this imprint remains unclear, but a rodent model
451 point towards transcriptomic reprogramming of monocytes in the spleen (5), while data from *in-*
452 *vitro* stimulated monocytes from a cohort in Mali point towards epigenetic reprogramming of
453 myeloid progenitor cells in the bone marrow (41). However, to our knowledge, no study has shown
454 that epigenetic remodeling can remain and affect innate cells at re-stimulation for that long.

455 An alternative hypothesis, that overcomes the fact that monocytes have a short lifespan (42), is
456 that they are remodeled in their function due to constant stimuli by remaining hemozoin in the
457 spleen (5, 43, 44).

458 Both hypotheses of epigenetic imprinting and through splenic remodeling need further
459 investigation. In our cohort, where study participants moved away from malaria endemic areas 10
460 years prior, we propose an additional mechanism responsible for the tolerogenic response via the
461 interplay of innate and adaptive immunity. We suggest that tolerance develops over several
462 exposures to parasites and further that it is sustained long-term through adaptive memory
463 responses. However, these above hypotheses are not mutually exclusive and could potentially
464 synergize.

465
466 In agreement with previous reports, we observed expanding $\gamma\delta$ T cells after the initial inflammatory
467 response in response to the infection (45, 46). $\gamma\delta$ T cells are suggested to have an important role in
468 the control of malaria (29) and direct anti-parasite functions during the blood stage have been
469 reported (24). In this study, we observed that the acute phase inflammatory response was positively
470 associated with expansion of $V\delta 2^+$ $\gamma\delta$ T cells, and further that this was strongly impacted by
471 previous malaria exposure, resulting in a dampened inflammatory response and less $\gamma\delta$ T cell
472 expansion. Interestingly, this effect was primarily observed for the subset of $V\delta 2^+$ and not $V\delta 2^-$
473 $\gamma\delta$ T cells. The strong association could indicate that the pro-inflammatory response directly or
474 indirectly shapes the subsequent $\gamma\delta$ T cell expansion and capacity to adapt to prolonged and high
475 levels of blood stage parasitemia.

476
477 $V\delta 2^+$ $\gamma\delta$ T cells are known to activate and expand during a primary *P. falciparum* infection in
478 response to malaria phosphoantigens and that their activity is modulated upon subsequent
479 infections (47). Given the recently described role of $V\delta 2^+$ $\gamma\delta$ T cells in antiparasitic activities via
480 antibody-CD16 dependent phagocytosis of infected erythrocytes and cytotoxicity (24, 25),
481 associations to possible activity modulating factors are of interest. The benefit of reduced
482 expansion of $\gamma\delta$ T cells due to a dampened inflammatory response could be to reduce overall
483 inflammatory responses, which are otherwise potentially detrimental to the host (48). This is a
484 common hypothesis as the $\gamma\delta$ T cells are known to acquire a dysfunctional or tolerance phenotype
485 over time with repeated episodes of malaria (23). This reduction in $\gamma\delta$ T cell effector function was
486 associated with continuous malaria exposure (23), although it remains unclear what the
487 underlying tolerance mechanism is, and how long-lived such an effect could be. To assess if the

488 reduced activation and expansion of V δ 2⁺ γ δ T cells could be due to an inherent inability of the γ δ
489 T cells to respond, we re-stimulated cells from primary infected and previously exposed
490 individuals. However, we did not observe any reduced response that could have been associated
491 with intrinsic down-regulation of effector functions. Based on this, we instead hypothesized that
492 the regulation of V δ 2⁺ γ δ T cell activation and expansion was likely due to extrinsic mechanisms.
493

494 Among the cytokines and chemokines associated with V δ 2⁺ γ δ T cell expansion, we found IFN-
495 gamma and CXCL11 significantly reduced in previously exposed individuals. CXCL11 is
496 chemotactic for activated T cells, and it was reported that individuals with asymptomatic
497 *P. falciparum* malaria had lower levels in an endemic setting (49). IFN-gamma and the IFN-
498 gamma inducible chemokine CXCL9 are associated in a different context with regulatory crosstalk
499 of pro-inflammatory γ δ T cell effects (50), which could explain the association of these cytokines
500 with subsequent expansion. Consistent with these observations, both IFN-gamma and CXCL11
501 were reduced due to previous parasite exposure in a mouse model, suggesting some type of
502 memory response (5).
503

504 In summary, our results, together with previous research in the field, supports a model where early
505 control of host self-damage through increased tolerance is needed until a more broad, diverse, and
506 protective antibody repertoire is achieved (see Figure 7G). The tolerance response (dampened pro-
507 inflammatory response and reduced V δ 2⁺ γ δ T cell expansion) could be mediated in two ways: 1)
508 an expanding antibody repertoire that enhances CD16⁺ mediated phagocytosis and effector
509 functions, direct parasite neutralization and blocking further RBC invasion, rosetting and
510 sequestration by merozoites, and 2) training/priming during previous malaria episodes via
511 epigenetic or transcriptional remodeling of the monocyte population, potentially leading to rapid
512 generation of CD16-expressing monocytes with enhanced antibody effector functions.
513

514 From an evolutionary perspective, this type of dampened inflammatory response could be
515 important to generate an efficient B cell response, as recently shown in an influenza vaccine study
516 (51) and further supported by mouse models of malaria (52). Although further studies are needed
517 to evaluate these mechanisms on a cellular and molecular level, the comprehensive systems levels

518 analysis performed here provides a dynamic description for how proteins, cells, and antibodies,
519 interact in the host response to malaria during and after primary and repeated infection.
520

521 MATERIALS AND METHODS

522 Study design/cohort

523 A prospective study enrolling adult patients diagnosed with *P. falciparum* malaria at Karolinska
524 University Hospital in Stockholm, Sweden. Fifty-three patients that were admitted with acute
525 *P. falciparum* infection between 2011 and 2017, and where both cells and plasma was frozen were
526 included in the current study. We stratified the patients based on previous exposure to compare the
527 immune responses in malaria-naïve individuals of primarily Swedish origin, who contracted
528 malaria for the first time (n = 17, denoted as primary infected), with individuals originating from
529 malaria-endemic areas in Sub-Saharan Africa and reporting previous malaria (n = 36, denoted as
530 previously exposed). Patients were invited for sampling at the time of malaria diagnosis (Acute)
531 and then at approximately 10 days (D10), 1 month (M1), 3 months (M3), 6 months (M6), and 12
532 months (Y1) (see Fig.1A). On each sampling, venous blood was collected for plasma and serum
533 isolation, PBMC preparation and blood chemistry. Peripheral blood mononuclear cells (PBMCs)
534 were isolated using Ficoll-Paque density gradient separation, resuspended in 90 % fetal calf serum
535 supplemented with 10% DMSO, and stored at - 150°C. Clinical data was extracted from medical
536 records, and a questionnaire relating to the participant's health status, previous traveling, and
537 malaria exposure was filled in by all participants (Table S1).

538 Part of the cohort has been described previously for clinical (53), parasitological (13) and
539 immunological aspects (15, 16, 54).

540 In addition, we profiled peripheral blood samples of eight healthy controls to compare relative
541 measures of protein expression and cell populations with healthy/normal values (Figure S2).

542

543 Clinical diagnostics

544 *P. falciparum* parasites were detected and enumerated by light microscopy of Fields stained thick
545 and thin blood smears at the Department of Clinical Microbiology at Karolinska University
546 Hospital in addition to PCR as described previously (13). Leukocyte, neutrophil, monocyte, and
547 platelet cell differential counts were performed at the Department of Clinical Chemistry at
548 Karolinska University Hospital.

549

550 **Data acquisition**

551 **Immune cell phenotyping**

552 Immune cells were phenotyped by Flow cytometry (LSRFortessa, BD) and a panel of 17 antibodies
553 covering major immune cell populations and subpopulations (Fig. S1) for 137 samples. Frozen
554 PBMCs were thawed in a 37°C water bath and mixed with 1 equal volume cold Iscove's Modified
555 Dulbecco's Medium supplemented with L-glutamine (2 mM), penicillin (100 U/ml), streptomycin
556 (100 µg/ml), and 10 % heat-inactivated fetal bovine serum (all from Thermo Fischer Scientific).
557 Cells were then rested 20 minutes on ice before being washed twice in DPBS lacking magnesium
558 or calcium. After washing, the cells were incubated with Aqua Live/Dead stain (Thermo Fisher
559 Scientific) for 20 minutes followed by further washing in DPBS supplemented with 2% FBS. The
560 cells were then incubated for 20 minutes on ice, in 2 steps with 2 washes in between, using an
561 antibody mix targeting surface antigens (Table S2). After staining, the cells were washed twice in
562 DPBS with 2% FBS before acquisition on a 5-laser BD LSRFortessa flow cytometer. Gating was
563 done with FlowJo X software version 10.4.2, with the gating strategy shown in Figure S1.

564 **Plasma protein profiling**

565 Plasma proteins relevant for the immune response were profiled using the Proximity Extension
566 Assay (PEA) (Olink Proteomics, Sweden) to analyze 171 samples of 53 individuals using Olink
567 Target 96 Inflammation panel (92-plex). The method has been described previously (17). Briefly,
568 paired oligonucleotide-coupled antibodies bind to target proteins, leading to hybridization of the
569 oligonucleotides when the antibody-pair is in close proximity, forming a PCR template for real-
570 time PCR detection. Resulting data is normalized using assay internal controls and transformed
571 into Normalized Protein eXpression (NPX) values, representing an arbitrary relative quantification
572 unit on log₂ scale. After quality control and removal of markers with a missing frequency greater
573 than 50%, 74 proteins remained for downstream analysis.

574

575 ***In vitro* stimulation for detection of $\gamma\delta$ T cells cytokine production**

576 For intracellular staining, PBMCs were thawed, washed, resuspended in complete RPMI media
577 supplemented with 10% FCS and then incubated at 37°C over-night. The cells were then
578 stimulated with PMA (0.4 µM) and ionomycin (13 µM) per 10⁶ cells, (Nordic Biosite AB) for 5
579 hours. Golgi plug (BD Biosciences) was added after the first hour of stimulation. Activated cells
580 were subsequently stained with antibodies targeting the surface markers CD3, $\gamma\delta$ TCR, and V δ 2,

581 according to manufacturers' instruction. Cells were then fixed and permeabilized using the BD
582 Cytotfix/Cytoperm reagents (BD Biosciences) and stained with intracellular antibodies for TNF,
583 IL17A, and IL10 (Table S2). For the exclusion of dead cells, LIVE/DEAD aqua fixable viability
584 staining kit (Invitrogen) was used. Cells were acquired using a BD LSR Fortessa BD (BD
585 Biosciences) and the data analyzed using FlowJo Version 7.6 (FlowJo, Ashland, OH).

586 **Bioinformatics**

587 **Immune cell data normalization**

588 Prior to bioinformatic analysis, cell proportions from manually gates (Fig. S1) were normalized to
589 the number of cells per 1000 live cells. Subsequently, we adjusted the experimentally obtained live
590 cell counts with lymphocyte and monocyte counts from clinical blood chemistry counts for each
591 individual and timepoint to obtain cells per microliter blood values (Fig. S5A). Monocyte gates
592 containing values (Fig. S1A) were normalized according to:

$$593 \quad \frac{\text{cells}}{1000 \text{ live cells}} * (\text{lymphocyte counts} + \text{monocyte counts}) = \frac{\text{cells}}{\text{microliter blood}}$$

594 Values of pure lymphocyte containing gates (Fig. S1B) were normalized according to:

$$595 \quad \frac{\text{cells}}{1000 \text{ live cells}} * \text{lymphocyte counts} = \frac{\text{cells}}{\text{microliter blood}}$$

596 To standardize the cells-per-microliter values and to normalize the data set for extreme values, we
597 performed log₂ transformation. Standardized data was comparable to not-standardized data (Fig.
598 S5B).

599 **Antibody cumulative response score (CRS) calculation**

600 A previous study on individuals of the traveler cohort investigated the immunoglobulin G subclass
601 response (IgG1-4) s to five malaria *P. falciparum*-blood-stage antigens (AMA1, MSP1, MSP2,
602 MSP3, RH5) in 52 this current study matching cohort individuals (15). For the current study, we
603 though to look at the overall IgG subclass response to merozoite antigens instead of specific
604 antigens. To summarize the adjusted signals, measured for each antigen and each subclass, we
605 rank normalized the signals to achieve normal distribution for each antigen (Fig. S5A). Normally
606 distributed antigen response values were then summarized for each IgG subclass and time point,
607 creating the cumulative response score (CRS), presenting an average breadth value of the antibody
608 response for IgG subclasses (Fig. S5B).

609

610 **Statistical analysis and visualization**

611

612 **Multi-Omics-Factor Analysis**

613 Multi-Omics Factor analysis (MOFA) is a powerful tool for omics integration. It reduces high-
614 dimensional data into a few latent factors by capturing multi-dataset spanning variance in these
615 factors. The unsupervised nature of MOFA+ allows the model to capture both biological and
616 technical variability in the low-dimensional factors space (18, 19). A recent development
617 (MEFISTO) in addition allows for multi-omics integration of data with continuous structures given
618 by temporal relationships(20). Here, we utilized MEFISTO to analyze the underlying key drivers
619 for the time course of one year after infection on our cohort of returning travelers with
620 *P. falciparum* malaria.

621 For the data-driven-integration approach, we used 15,396 immune feature data points out of 23,130
622 possible. We included manually gated immune cell subset (features = 44) data and highly
623 multiplexed plasma protein data (features = 60) and including the time after symptom onset (0-70
624 weeks) for each sample to disentangle time dependent variation on a systems-level.

625 To standardize the actual time covariate of each sample, we used the time after reported symptom
626 onset for each sample as a temporal covariate for the model. Moreover, we assigned the time-
627 associated samples to groups of primary infected (n = 57) and previously exposed (n = 125) to
628 account for previous *P. falciparum* exposure. Immune parameters without temporal variation were
629 excluded prior to model training.

630 We trained the MEFISTO model using default model options, but adjusted training options (drop-
631 factor-threshold = 0.05; maxiter = 10,000; convergence_mode = slow). To align the covariates
632 across groups, warping was set “TRUE” and “primary infected” was set as warping reference
633 group. The optimal model was determined by the MOFA+ function `run_mofa()` with the setting
634 “use_basilisk = T”.

635

636 All data wrangling, analysis and visualization was done using R (www.r-project.org) using the
637 tidyverse package (55). Spearman correlation analysis with FDR/BH correction for multiple
638 testing (56) was done using the correlation package (57). If not stated otherwise, non-parametric
639 data distribution was assumed, and statistical difference was assessed using unpaired Wilcoxon Test
640 from `rstatix` (<https://github.com/kassambara/rstatix>).

641 Results were visualized using r packages circlize (58), complexHeatmap (59) and ggpubr
642 (<https://github.com/kassambara/ggpubr9>). Linear-mixed-effect models, with subjectID as random
643 effect, were fitted in GraphPad prism version 9.1.2 using restricted maximum likelihood followed
644 by t-tests using predicted least squares means with Benjamini and Hochberg FDR correction for
645 multiple testing (56).

646

647 **Supplementary Materials**

648 Table S1. Descriptive statistics prospective cohort of returning travelers.

649 Table S2. Staining panel for flow cytometry

650 Fig. S1. Flow cytometry manual gating strategy – T cell and B cell panel.

651 Fig. S2. MEFISTO model and cohort internal feature evaluation.

652 Fig. S3. Cohort external evaluation - comparison of plasma protein and PBMC profiles at Acute
653 and Y1 compared to healthy controls.

654 Fig. S4. Comparison of MEFISTO Factor1 values for exposure groups on time points.

655 Fig. S5. Cumulative Response Score for malaria antigen specific IgG subclass response of Yman
656 et al 2019 data set.

657 Fig. S6. Leukocyte count adjusted cell counts.

658 Fig. S7. Directed Acyclic Graphs – DAGs and linear regression

659

660 **References and Notes**

661 1. World Health Organisation, *World malaria report 2020* (Geneva, 2020);

662 <https://www.who.int/teams/global-malaria-programme/reports/world-malaria-report-2020>).

663 2. J. Langhorne, F. M. Ndungu, A. M. Sponaas, K. Marsh, Immunity to malaria: More questions
664 than answers *Nature Immunology* **9**, 725–732 (2008).

665 3. F. H. A. Osier, G. Fegan, S. D. Polley, L. Murungi, F. Verra, K. K. A. Tetteh, B. Lowe, T.

666 Mwangi, P. C. Bull, A. W. Thomas, D. R. Cavanagh, J. S. McBride, D. E. Lanar, M. J.

667 Mackinnon, D. J. Conway, K. Marsh, Breadth and magnitude of antibody responses to multiple

- 668 Plasmodium falciparum merozoite antigens are associated with protection from clinical malaria,
669 *Infection and Immunity* (2008), doi:10.1128/IAI.01585-07.
- 670 4. B. P. Gonçalves, C.-Y. Huang, R. Morrison, S. Holte, E. Kabyemela, D. R. Prevots, M. Fried,
671 P. E. Duffy, Parasite Burden and Severity of Malaria in Tanzanian Children, *New England*
672 *Journal of Medicine* **370**, 1799–1808 (2014).
- 673 5. W. Nahrendorf, A. Ivens, P. J. Spence, Inducible mechanisms of disease tolerance provide an
674 alternative strategy of acquired immunity to malaria, *eLife* **10** (2021), doi:10.7554/eLife.63838.
- 675 6. A. F. Cowman, J. Healer, D. Marapana, K. Marsh, Malaria: Biology and Disease *Cell* **167**,
676 610–624 (2016).
- 677 7. P. D. Crompton, J. Moebius, S. Portugal, M. Waisberg, G. Hart, L. S. Garver, L. H. Miller, C.
678 Barillas-Mury, S. K. Pierce, Malaria Immunity in Man and Mosquito: Insights into Unsolved
679 Mysteries of a Deadly Infectious Disease, *Annual Review of Immunology* **32**, 157–187 (2014).
- 680 8. C. Loiseau, M. M. Cooper, D. L. Doolan, Deciphering host immunity to malaria using systems
681 immunology, *Immunological Reviews* **293**, 115–143 (2020).
- 682 9. T. M. Tran, P. D. Crompton, Decoding the complexities of human malaria through systems
683 immunology *Immunological Reviews* **293**, 144–162 (2020).
- 684 10. M. M. Davis, C. M. Tato, D. Furman, Systems immunology: Just getting started *Nature*
685 *Immunology* **18**, 725–732 (2017).
- 686 11. T. M. Tran, R. Guha, S. Portugal, J. Skinner, A. Ongoiba, J. Bhardwaj, M. Jones, J. Moebius,
687 P. Venepally, S. Doumbo, E. A. DeRiso, S. Li, K. Vijayan, S. L. Anzick, G. T. Hart, E. M.
688 O’Connell, O. K. Doumbo, A. Kaushansky, G. Alter, P. L. Felgner, H. Lorenzi, K. Kayentao, B.
689 Traore, E. F. Kirkness, P. D. Crompton, A Molecular Signature in Blood Reveals a Role for p53
690 in Regulating Malaria-Induced Inflammation, *Immunity* (2019),
691 doi:10.1016/J.IMMUNI.2019.08.009.
- 692 12. S. E. Jong, V. Unen, M. D. Manurung, K. A. Stam, J. J. Goeman, S. P. Jochems, T. Hamp, N.
693 Pezzotti, Y. D. Mouwenda, M. Eunice Betouke Ongwe, F.-R. Lorenz, Y. C. M Kruize, S. Azimi,
694 M. H. Kamp, A. Vilanova, E. Eisemann, B. P. F Lelieveldt, M. Roestenberg, B. Kim Lee Sim,
695 M. J. T Reinders, R. Fendel, S. L. Hoffman, P. G. Kremsner, F. Koning, B. Mordmamp, B. Lell,
696 M. Yazdanbakhsh, Systems analysis and controlled malaria infection in Europeans and Africans
697 elucidate naturally acquired immunity, *Nature Immunology* (2021), doi:10.1038/s41590-021-
698 00911-7.

- 699 13. M. Vafa Homann, S. N. Emami, V. Yman, C. Stenström, K. Sondén, H. Ramström, M.
700 Karlsson, M. Asghar, A. Färnert, Detection of Malaria Parasites After Treatment in Travelers: A
701 12-months Longitudinal Study and Statistical Modelling Analysis, *EBioMedicine* **25**, 66–72
702 (2017).
- 703 14. M. Asghar, V. Yman, M. V. Homann, K. Sondén, U. Hammar, D. Hasselquist, A. Färnert,
704 Cellular aging dynamics after acute malaria infection: A 12-month longitudinal study, *Aging Cell*
705 (2018), doi:10.1111/accel.12702.
- 706 15. V. Yman, M. T. White, M. Asghar, C. Sundling, K. Sondén, S. J. Draper, F. H. A. A. Osier,
707 A. Färnert, Antibody responses to merozoite antigens after natural *Plasmodium falciparum*
708 infection: Kinetics and longevity in absence of re-exposure, *BMC Medicine* (2019),
709 doi:10.1186/s12916-019-1255-3.
- 710 16. C. Sundling, C. Rönnerberg, V. Yman, M. Asghar, P. Jahnmatz, T. Lakshmikanth, Y. Chen, J.
711 Mikes, M. N. Forsell, K. Sondén, A. Achour, P. Brodin, K. E. M. Persson, A. Färnert, B cell
712 profiling in malaria reveals expansion and remodeling of CD11c⁺ B cell subsets, *JCI Insight*
713 (2019), doi:10.1172/jci.insight.126492.
- 714 17. E. Assarsson, M. Lundberg, G. Holmquist, J. Björkesten, S. Bucht Thorsen, D. Ekman, A.
715 Eriksson, E. Rennel Dickens, S. Ohlsson, G. Edfeldt, A.-C. Andersson, P. Lindstedt, J. Stenvang,
716 M. Gullberg, S. Fredriksson, J. D. Hoheisel, Ed. Homogenous 96-Plex PEA Immunoassay
717 Exhibiting High Sensitivity, Specificity, and Excellent Scalability, *PLoS ONE* **9**, e95192 (2014).
- 718 18. R. Argelaguet, B. Velten, D. Arnol, S. Dietrich, T. Zenz, J. C. Marioni, F. Buettner, W.
719 Huber, O. Stegle, Multi-Omics Factor Analysis—a framework for unsupervised integration of
720 multi-omics data sets, *Molecular Systems Biology* (2018), doi:10.15252/msb.20178124.
- 721 19. R. Argelaguet, D. Arnol, D. Bredikhin, Y. Deloro, B. Velten, J. C. Marioni, O. Stegle,
722 MOFA+: A statistical framework for comprehensive integration of multi-modal single-cell data,
723 *Genome Biology* **21**, 111 (2020).
- 724 20. B. Velten, J. M. Braunger, D. Arnol, R. Argelaguet, O. Stegle, Identifying temporal and
725 spatial patterns of variation from multi-modal data using MEFISTO, ,
726 doi:10.1101/2020.11.03.366674.
- 727 21. P. Jagannathan, F. Lutwama, M. J. Boyle, F. Nankya, L. A. Farrington, T. I. McIntyre, K.
728 Bowen, K. Naluwu, M. Nalubega, K. Musinguzi, E. Sikyomu, R. Budker, A. Katureebe, J. Rek,
729 B. Greenhouse, G. Dorsey, M. R. Kanya, M. E. Feeney, Vδ2⁺ T cell response to malaria

- 730 correlates with protection from infection but is attenuated with repeated exposure, *Scientific*
731 *Reports* **7**, 1–12 (2017).
- 732 22. L. A. Farrington, P. C. Callaway, H. M. Vance, K. Baskevitch, E. Lutz, L. Warriar, T. I.
733 McIntyre, R. Budker, P. Jagannathan, F. Nankya, K. Musinguzi, M. Nalubega, E. Sikyomu, K.
734 Naluwu, E. Arinaitwe, G. Dorsey, M. R. Kamya, M. E. Feeney, G. Hart, Ed. Opsonized antigen
735 activates V δ 2+ T cells via CD16/FC γ RIIIa in individuals with chronic malaria exposure, *PLOS*
736 *Pathogens* **16**, e1008997 (2020).
- 737 23. P. Jagannathan, C. C. Kim, B. Greenhouse, F. Nankya, K. Bowen, I. Eccles-James, M. K.
738 Muhindo, E. Arinaitwe, J. W. Tappero, M. R. Kamya, G. Dorsey, M. E. Feeney, Loss and
739 dysfunction of V δ 2+ γ δ T cells are associated with clinical tolerance to malaria, *Science*
740 *Translational Medicine* **6**, 251ra117-251ra117 (2014).
- 741 24. C. Junqueira, R. B. Polidoro, G. Castro, S. Absalon, Z. Liang, S. sen Santara, Â. Crespo, D.
742 B. Pereira, R. T. Gazzinelli, J. D. Dvorin, J. Lieberman, γ δ T cells suppress Plasmodium
743 falciparum blood-stage infection by direct killing and phagocytosis, *Nature Immunology* , 1–11
744 (2021).
- 745 25. L. A. Farrington, P. C. Callaway, H. M. Vance, K. Baskevitch, E. Lutz, L. Warriar, T. I.
746 McIntyre, R. Budker, P. Jagannathan, F. Nankya, K. Musinguzi, M. Nalubega, E. Sikyomu, K.
747 Naluwu, E. Arinaitwe, G. Dorsey, M. R. Kamya, M. E. Feeney, G. Hart, Ed. Opsonized antigen
748 activates V δ 2+ T cells via CD16/FC γ RIIIa in individuals with chronic malaria exposure, *PLOS*
749 *Pathogens* **16**, e1008997 (2020).
- 750 26. H. H. van Acker, A. Capsomidis, E. L. Smits, V. F. van Tendeloo, CD56 in the immune
751 system: More than a marker for cytotoxicity? *Frontiers in Immunology* **8**, 1 (2017).
- 752 27. W. Xu, A. Larbi, Heterogeneity in V δ 2pos T cell homeostasis in response to
753 stress *EBioMedicine* **43**, 31 (2019).
- 754 28. V. Appay, R. A. W. van Lier, F. Sallusto, M. Roederer, Phenotype and function of human T
755 lymphocyte subsets: Consensus and issues *Cytometry Part A* **73**, 975–983 (2008).
- 756 29. K. Deroost, J. Langhorne, Gamma/Delta T Cells and Their Role in Protection Against
757 Malaria, *Frontiers in Immunology* **9**, 2973 (2018).
- 758 30. H. Hsu, S. Boudova, G. Mvula, T. H. Divala, R. G. Mungwira, C. Harman, M. K. Laufer, C.
759 D. Pauza, C. Cairo, Prolonged PD1 Expression on Neonatal V δ 2 Lymphocytes Dampens

- 760 Proinflammatory Responses: Role of Epigenetic Regulation, *The Journal of Immunology* **197**,
761 1884–1892 (2016).
- 762 31. K. W. Dantzler, P. Jagannathan, $\gamma\delta$ T cells in antimalarial immunity: New insights into their
763 diverse functions in protection and tolerance *Frontiers in Immunology* (2018),
764 doi:10.3389/fimmu.2018.02445.
- 765 32. A. Ankan, I. M. N. Wortel, J. Textor, Testing Graphical Causal Models Using the R Package
766 “dagitty,” *Current Protocols* **1** (2021), doi:10.1002/cpz1.45.
- 767 33. T. W. Ademolue, Y. Aniweh, K. A. Kusi, G. A. Awandare, Patterns of inflammatory
768 responses and parasite tolerance vary with malaria transmission intensity, *Malaria Journal* **16**,
769 145 (2017).
- 770 34. T. M. Tran, M. B. Jones, A. Ongoiba, E. M. Bijker, R. Schats, P. Venepally, J. Skinner, S.
771 Doumbo, E. Quinten, L. G. Visser, E. Whalen, S. Presnell, E. M. O’connell, K. Kayentao, O. K.
772 Doumbo, D. Chaussabel, H. Lorenzi, T. B. Nutman, T. H. M. Ottenhoff, M. C. Haks, B. Traore,
773 E. F. Kirkness, R. W. Sauerwein, P. D. Crompton, Transcriptomic evidence for modulation of
774 host inflammatory responses during febrile *Plasmodium falciparum* malaria OPEN, (2016),
775 doi:10.1038/srep31291.
- 776 35. L. Farrington, H. Vance, J. Rek, M. Prah, P. Jagannathan, A. Katureebe, E. Arinaitwe, M. R.
777 Kanya, G. Dorsey, M. E. Feeney, Both inflammatory and regulatory cytokine responses to
778 malaria are blunted with increasing age in highly exposed children, *Malaria Journal* **16**, 499
779 (2017).
- 780 36. P. Jahnmatz, C. Sundling, V. Yman, L. Widman, M. Asghar, K. Sondén, C. Stenström, C.
781 Smedman, F. Ndungu, N. Ahlborg, A. Färnert, Memory B-Cell Responses Against Merozoite
782 Antigens After Acute *Plasmodium falciparum* Malaria, Assessed Over One Year Using a Novel
783 Multiplexed FluoroSpot Assay, *Frontiers in Immunology* **11**, 619398 (2021).
- 784 37. F. M. Ndungu, K. Lundblom, J. Rono, J. Illingworth, S. Eriksson, A. Färnert, Long-lived
785 *Plasmodium falciparum* specific memory B cells in naturally exposed Swedish travelers,
786 *European Journal of Immunology* (2013), doi:10.1002/eji.201343630.
- 787 38. A. Ortega-Pajares, S. J. Rogerson, The Rough Guide to Monocytes in Malaria
788 Infection *Frontiers in immunology* **9**, 2888 (2018).
- 789 39. S. P. Kurup, N. S. Butler, J. T. Harty, T cell-mediated immunity to malaria *Nature Reviews*
790 *Immunology* **19**, 457–471 (2019).

- 791 40. T. J. Suscovich, J. K. Fallon, J. Das, A. R. Demas, J. Crain, C. H. Linde, A. Michell, H.
792 Natarajan, C. Arevalo, T. Broge, T. Linnekin, V. Kulkarni, R. Lu, M. D. Slein, C. Luedemann,
793 M. Marquette, S. March, J. Weiner, S. Gregory, M. Coccia, Y. Flores-Garcia, F. Zavala, M. E.
794 Ackerman, E. Bergmann-Leitner, J. Hendriks, J. Sadoff, S. Dutta, D. A. Lauffenburger, E.
795 Jongert, U. Wille-Reece, G. Alter, *Mapping functional humoral correlates of protection against*
796 *malaria challenge following RTS,S/AS01 vaccination* (2020).
- 797 41. R. Guha, A. Mathioudaki, S. Doumbo, D. Doumtabe, J. Skinner, G. Arora, S. Siddiqui, S. Li,
798 K. Kayentao, A. Ongoiba, J. Zaugg, B. Traore, P. D. Crompton, J. W. Kazura, Ed. Plasmodium
799 falciparum malaria drives epigenetic reprogramming of human monocytes toward a regulatory
800 phenotype, *PLOS Pathogens* **17**, e1009430 (2021).
- 801 42. A. A. Patel, Y. Zhang, J. N. Fullerton, L. Boelen, A. Rongvaux, A. A. Maini, V. Bigley, R.
802 A. Flavell, D. W. Gilroy, B. Asquith, D. Macallan, S. Yona, The fate and lifespan of human
803 monocyte subsets in steady state and systemic inflammation, *Journal of Experimental Medicine*
804 **214**, 1913–1923 (2017).
- 805 43. P. A. Buffet, I. Safeukui, G. Deplaine, V. Brousse, V. Prendki, M. Thellier, G. D. Turner, O.
806 Mercereau-Puijalon, The pathogenesis of Plasmodium falciparum malaria in humans: Insights
807 from splenic physiology *Blood* **117**, 381–392 (2011).
- 808 44. S. Kho, L. Qotrunnada, L. Leonardo, B. Andries, P. A. I. Wardani, A. Fricot, B. Henry, D.
809 Hardy, N. I. Margyaningsih, D. Apriyanti, A. M. Puspitasari, P. Prayoga, L. Trianty, E.
810 Kenangalem, F. Chretien, I. Safeukui, H. A. del Portillo, C. Fernandez-Becerra, E. Meibalan, M.
811 Marti, R. N. Price, T. Woodberry, P. A. Ndour, B. M. Russell, T. W. Yeo, G. Minigo, R.
812 Noviyanti, J. R. Poespoprodjo, N. C. Siregar, P. A. Buffet, N. M. Anstey, Hidden Biomass of
813 Intact Malaria Parasites in the Human Spleen, *New England Journal of Medicine* **384**, 2067–
814 2069 (2021).
- 815 45. M. R. Mamedov, A. Scholzen, R. v. Nair, K. Cumnock, J. A. Kenkel, J. H. M. Oliveira, D. L.
816 Trujillo, N. Saligrama, Y. Zhang, F. Rubelt, D. S. Schneider, Y. hsiu Chien, R. W. Sauerwein,
817 M. M. Davis, A Macrophage Colony-Stimulating-Factor-Producing $\gamma\delta$ T Cell Subset Prevents
818 Malarial Parasitemic Recurrence, *Immunity* **48**, 350-363.e7 (2018).
- 819 46. A. Trampuz, M. Jereb, I. Muzlovic, R. M. Prabhu, Clinical review: Severe malaria *Critical*
820 *Care* **7**, 315–323 (2003).

- 821 47. J. Howard, I. Zaidi, S. Loizon, O. Mercereau-Puijalon, J. Déchanet-Merville, M. Mamani-
822 Matsuda, Human V γ 9V δ 2 T Lymphocytes in the Immune Response to *P. falciparum* Infection,
823 *Frontiers in Immunology* **9**, 2760 (2018).
- 824 48. D. I. Stanisic, J. Cutts, E. Eriksson, F. J. I. Fowkes, A. Rosanas-Urgell, P. Siba, M. Laman,
825 T. M. E. Davis, L. Manning, I. Mueller, L. Schofield, $\gamma\delta$ T cells and CD14⁺ Monocytes Are
826 Predominant Cellular Sources of Cytokines and Chemokines Associated With Severe Malaria,
827 *The Journal of Infectious Diseases* **210**, 295–305 (2014).
- 828 49. J. N. Che, O. P. G. Nmorsi, B. P. Nkot, C. Isaac, B. C. Okonkwo, Chemokines responses to
829 *Plasmodium falciparum* malaria and co-infections among rural Cameroonians, *Parasitology*
830 *International* **64**, 139–144 (2015).
- 831 50. M. N. Ajuebor, Y. Jin, G. L. Gremillion, R. M. Strieter, Q. Chen, P. A. Adegboyega, $\gamma\delta$ T
832 Cells Initiate Acute Inflammation and Injury in Adenovirus-Infected Liver via Cytokine-
833 Chemokine Cross Talk, *Journal of Virology* **82**, 9564–9576 (2008).
- 834 51. D. L. Hill, S. Innocentin, J. Wang, E. A. James, J. C. Lee, W. Kwok, M. Zand, E. J. Carr, M.
835 A. Linterman, Impaired HA-specific T follicular helper cell and antibody responses to, ,
836 doi:10.1101/2021.04.07.21255038.
- 837 52. V. Ryg-Cornejo, L. J. Ioannidis, A. Ly, C. Y. Chiu, J. Tellier, D. L. Hill, S. P. Preston, M.
838 Pellegrini, D. Yu, S. L. Nutt, A. Kallies, D. S. Hansen, Severe Malaria Infections Impair
839 Germinal Center Responses by Inhibiting T Follicular Helper Cell Differentiation, *Cell Reports*
840 **14**, 68–81 (2016).
- 841 53. K. Sondén, K. Wyss, I. Jovel, A. Vieira Da Silva, A. Pohanka, M. Asghar, M. V. Homann, L.
842 L. Gustafsson, U. Hellgren, A. Färnert, High Rate of Treatment Failures in Nonimmune
843 Travelers Treated With Artemether-Lumefantrine for Uncomplicated *Plasmodium falciparum*
844 Malaria in Sweden: Retrospective Comparative Analysis of Effectiveness and Case Series,
845 *Clinical Infectious Diseases Malaria Treatment Failures in Travelers • CID* **2017**, 199–206.
- 846 54. M. Asghar, V. Yman, M. V. Homann, K. Sondén, U. Hammar, D. Hasselquist, A. Färnert,
847 Cellular aging dynamics after acute malaria infection: A 12-month longitudinal study, *Aging Cell*
848 **17**, e12702 (2018).
- 849 55. H. Wickham, M. Averick, J. Bryan, W. Chang, L. D', A. McGowan, R. François, G.
850 Grolemond, A. Hayes, L. Henry, J. Hester, M. Kuhn, T. Lin Pedersen, E. Miller, S. M. Bache, K.
851 Müller, J. Ooms, D. Robinson, D. P. Seidel, V. Spinu, K. Takahashi, D. Vaughan, C. Wilke, K.

852 Woo, H. Yutani, RStudio 2 cynkra 3 Redbubble 4 Erasmus University Rotterdam 5 Flatiron
853 Health 6 Department of Integrative Biology, *Journal of Open Source Software* **4**, 1686 (2019).
854 56. Y. Benjamini, Y. Hochberg, Controlling the False Discovery Rate: A Practical and Powerful
855 Approach to Multiple Testing, *Journal of the Royal Statistical Society: Series B*
856 (*Methodological*) **57**, 289–300 (1995).
857 57. D. Makowski, M. Ben-Shachar, I. Patil, D. Lüdtke, Methods and Algorithms for
858 Correlation Analysis in R, *Journal of Open Source Software* **5**, 2306 (2020).
859 58. Z. Gu, L. Gu, R. Eils, M. Schlesner, B. Brors, Genome analysis circlize implements and
860 enhances circular visualization in R, **30**, 2811–2812 (2014).
861 59. Z. Gu, R. Eils, M. Schlesner, Complex heatmaps reveal patterns and correlations in
862 multidimensional genomic data, *Bioinformatics* (2016), doi:10.1093/bioinformatics/btw313.
863 60. FOR THE TREATMENT OF MALARIA GUIDELINES, (2015) (available at
864 www.who.int).

865

866

867

868

869 **Acknowledgments:**

870 We would firstly like to acknowledge the contribution of all the study participants. We would
871 also like to thank all involved clinicians, nurses especially Irene Nordling and Debbie Ribjer for
872 sampling and Fariba Foroogh for sample processing and organization. Further, we would like to
873 thank the team from the Translational Plasma Profile Facility at SciLifeLab for support and the
874 generation of data for this project. Figure 1A and 7G were created with BioRender.com.

875 **Funding:**

876 The Swedish Research Council grant 2019-01940 (CS)
877 Magnus Bergvall foundation grant 2017-02043 and 2018-02656 (CS)
878 Åke Wiberg foundation grant M18-0076 (CS)
879 Swedish Research Council 2015-02977, 2018-02688 and 2018-04468 (AF)
880 Region Stockholm 20150135 and 20180409 (AF)
881 Marianne and Marcus Wallenberg Foundation (AF)

882 **Author contributions:**

883 Conceptualization: CS, MJL, AF
884 Methodology: CS, MJL, NK, SA
885 Investigation: CS, MJL, KS, VY, NK, SA, DFP, AF
886 Visualization: CS, MJL
887 Funding acquisition: CS, AF
888 Project administration: CS
889 Supervision: CS, AF
890 Writing – original draft: CS, MJL
891 Writing – review & editing: CS, MJL, AF, KS, VY, NK, SA, DFP

892 **Competing interests:**

893 Authors declare that they have no competing interests.

894 **Data and materials availability:**

895 The flow cytometry data and plasma protein data (Olink Inflammation panel) generated during
896 this study are available upon request. Code used in the analyzes is available in repository:
897 <https://github.com/LautenbachMJ/MalariaTraveller>.